

Low temperature sintering of Ag nanoparticles for flexible electronics packaging

A. Hu, J. Y. Guo, H. Alarifi, G. Patane, Y. Zhou, G. Compagnini, and C. X. Xu

Citation: [Applied Physics Letters](#) **97**, 153117 (2010); doi: 10.1063/1.3502604

View online: <http://dx.doi.org/10.1063/1.3502604>

View Table of Contents: <http://scitation.aip.org/content/aip/journal/apl/97/15?ver=pdfcov>

Published by the [AIP Publishing](#)

Articles you may be interested in

[Size and alloying induced changes in lattice constant, core, and valance band binding energy in Pd-Ag, Pd, and Ag nanoparticles: Effect of in-flight sintering temperature](#)

[J. Appl. Phys.](#) **112**, 014307 (2012); 10.1063/1.4731714

[High thermal conductivity epoxy-silver composites based on self-constructed nanostructured metallic networks](#)

[J. Appl. Phys.](#) **111**, 104310 (2012); 10.1063/1.4716179

[Micro-ink-jetting of silver nanoparticles on low temperature cofired ceramic substrates for drop-on-demand metallization](#)

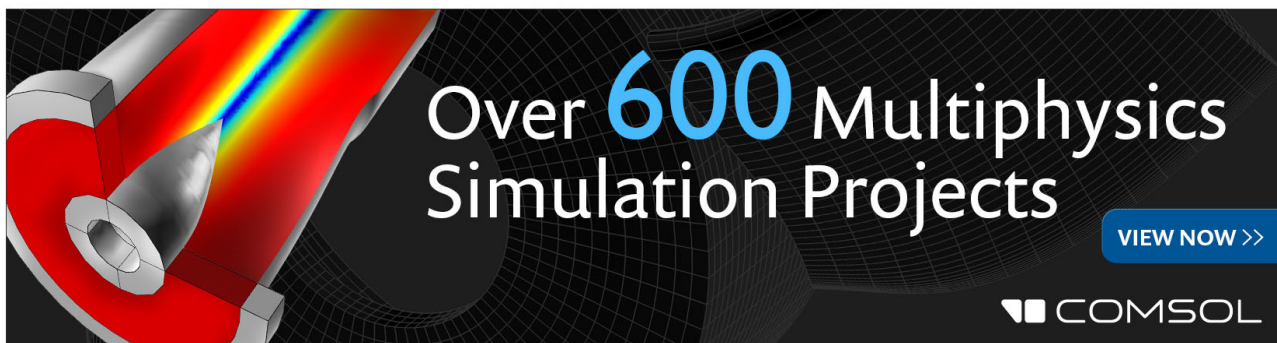
[J. Vac. Sci. Technol. B](#) **27**, 1431 (2009); 10.1116/1.3093921

[Air-stable inverted flexible polymer solar cells using zinc oxide nanoparticles as an electron selective layer](#)

[Appl. Phys. Lett.](#) **92**, 253301 (2008); 10.1063/1.2945281

[Organic-transistor-based flexible pressure sensors using ink-jet-printed electrodes and gate dielectric layers](#)

[Appl. Phys. Lett.](#) **89**, 253507 (2006); 10.1063/1.2416001

The advertisement features a dark background with a grid pattern. On the left, there is a 3D cutaway illustration of a mechanical part with a red and yellow color gradient. The text 'Over 600 Multiphysics Simulation Projects' is prominently displayed in white and blue. A blue button with the text 'VIEW NOW >>' is located on the right. The COMSOL logo is in the bottom right corner.

Over **600** Multiphysics Simulation Projects

[VIEW NOW >>](#)

COMSOL

Low temperature sintering of Ag nanoparticles for flexible electronics packaging

A. Hu,^{1,a)} J. Y. Guo,² H. Alarifi,¹ G. Patane,³ Y. Zhou,¹ G. Compagnini,³ and C. X. Xu²

¹Department of Mechanical and Mechatronics Engineering, Centre for Advanced Material Joining, University of Waterloo, 200 University Avenue West, Waterloo, Ontario N2L 3G1, Canada

²State Key Laboratory of Bioelectronics, Advanced Photonics Center, Southeast University, Nanjing 210096, People's Republic of China

³Dipartimento di Scienze Chimiche, Università di Catania, Viale A. Doria 6, Catania 95125, Italy

(Received 24 August 2010; accepted 25 September 2010; published online 13 October 2010)

We achieve robust bonding of Cu wires to Cu pads on polyimide with silver nanopaste cured at 373 K. The paste is prepared by simply condensing Ag nanoparticle (NP) solution via centrifuging. The bonding is formed by solid state sintering of Ag NPs through neck growth and direct metallic bonding between clean Ag–Cu interfaces. Both experiment and Monte Carlo simulation confirm that the melting point of joint clusters increases during sintering. This creates improved bonds for use at an elevated operating temperature using Ag NPs. © 2010 American Institute of Physics.

[doi:10.1063/1.3502604]

There is increasing interest in developing low temperature interconnection processes for flexible electronics, including flat-panel displays, organic electronics, and low-cost disposable microelectronic devices on plastic substrates.^{1–4} These substrates, such as poly(ethyleneterephthalate), polyimide, and paper, as well as some electronic components based on organic groups or nanosized building blocks, cannot maintain their functions and stabilities at a temperature range of 473–573 K, which is required for melting lead-free solders extensively used in microelectronics soldering and reflow.^{1,5–7} On the other hand, higher power chips, e.g., central processing units, and automotive electronics near the engine, frequently work at a temperature near 473 K.^{8,9} An advanced bonding technology, which allows a low temperature curing but withstands a higher working temperature, is thus desired.

Silver nanoparticle (NP) paste has been developed through metallo-organic decomposition to avoid unstable contact resistance and low working temperature of conventional electronically conductive adhesives with silver NP addition.^{9,10} Ag NP paste has been shown to be capable of bonding and curing at low temperatures ranging from 473 to 573 K.^{3–5,9,11} In this paper, we report a silver paste directly condensed from silver NP solution through centrifugation. Robust bonding of Cu wires to Cu pads on polyimide has been realized at a temperature of 373 K, sufficiently low for flexible electronics. The experiments show that this low temperature curing paste can work at a higher temperature than the sintering temperature with enhanced bond strength.

A 1 mM solution of silver NPs was prepared by reduction of silver nitride with sodium citrate at a temperature of about 363 K.¹² Condensation was carried out with a centrifuge at 4000 rpm for 30 min. The concentration of silver in the resulting paste was about 0.2 M. These Ag NPs were deposited on silicon wafers for scanning electron microscopy (SEM) and x-ray photoelectron spectroscopy (XPS). The bonding of Cu wires to Cu pads was conducted with Ag paste at 5 MPa pressure at different curing temperatures.

Prior to bonding the surfaces of the Cu pads were cleaned in ultrasonic bath with acetone. Transmission electron microscopy (TEM) has been performed on cross-sectional samples cut with microtomy.

Figure 1(a) shows a SEM micrograph of condensed Ag NPs. Most of the Ag NPs are spherical. The mean size of the NPs is about 50 nm. It is clearly visible that Ag NPs are still well separated after condensation. This phenomenon is clarified in detailed TEM investigation. Figure 1(b) displays a typical Ag NP deposited on formvar coated TEM copper grids. An amorphous organic shell with a thickness of 1 nm is clearly visible. It is reasonable to deduce that this shell prevents the coalescence of Ag NPs. Shown in Fig. 1(c) is an SEM image of Ag NPs sintered at 523 K for 3 min. The bonding is evident by the formation of the necked connections between Ag NPs. The bridging paths occur between neighboring Ag NPs, orient arbitrarily, and eventually generates a three-dimensional (3D) connection network. These joints are not a result of melting of the particles because these NPs are expected to melt at a temperature ranging of 673–873 K based on the size effect,¹³ far above the present

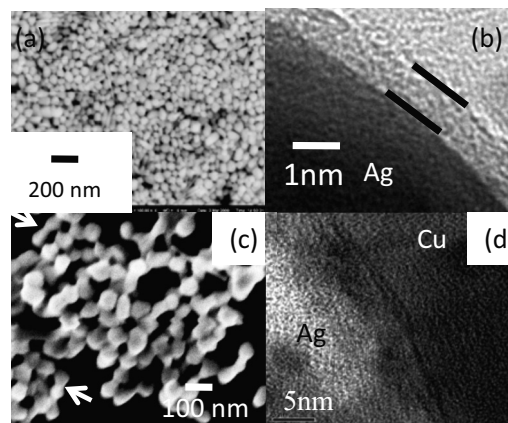


FIG. 1. (a) SEM images of condensed Ag NPs. (b) TEM images of a typical Ag NP. Two lines indicate the boundaries of organic shells. (c) SEM image of Ag NPs sintered at 250 °C for 3 min. (d) TEM images of the bonding interfaces between Ag NPs and Cu pads at curing temperature of 523 K.

^{a)}Electronic mail: a2hu@unwaterloo.ca.

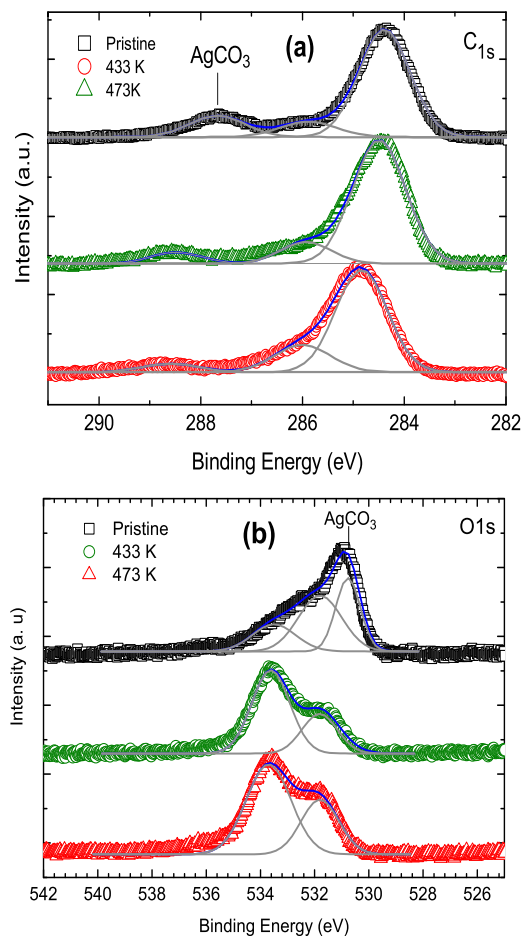


FIG. 2. (Color online) Binding energy levels of (a) C $1s$ and (b) O $1s$ lines for pristine Ag NPs and two sintered samples, one at 433 K for 5 min and the other at 473 K for 5 min, respectively. Solid lines correspond to fitting by Gaussian line shapes.

sintering temperature. The solid state coalescence arising from surface atom diffusion may be the bonding mechanism between these NPs. Figure 1(d) shows TEM images of the bonding interface between Ag NPs and Cu pads at curing temperature of 523 K. Direct metallic bonding is evident. There is no distinguishable intermediate disorder layer in spite of the significant lattice mismatch between Cu and Ag. A clear contrast belt with a thickness less than 1 nm is evident in the interface. This may indicate the concentration of local stress. These results are significantly different from the bonding using Ag metallo-organic compounds,^{3,8,11} where a disordered lattice layer of 1–3 nm has been clearly observed. This difference may arise from the different thicknesses and components of the organic shell.

Figure 2 exhibits the (a) C $1s$ and (b) O $1s$ lines of XPS for pristine Ag NPs and two samples, sintered at 433 K for 5 min and at 473 K for 5 min, respectively. The deconvoluted analysis yields C $1s$ binding energy levels and O $1s$ binding energy levels at variable groups. C $1s$ is identified in $-\text{COO}^-$ group at 288.5 eV, Ag_2CO_3 at 287.7 eV and alcoholic $-\text{COH}$ group at 285.5 eV besides aliphatic carbon at 284.4–284.8 eV.^{14,15} Meanwhile, O $1s$ is determined in $-\text{COO}^-$ at 533.6 eV, in $-\text{COH}$ at 531.8 eV, and 530.8 eV in Ag_2CO_3 .^{14,16,17} There are no remarkable contributions of O $1s$ from Ag_2O or AgO for all three samples because both of them display Ag binding energy levels lower than 530 eV.^{14,17} This may indicate that Ag does not exist in an oxide state in the present composi-

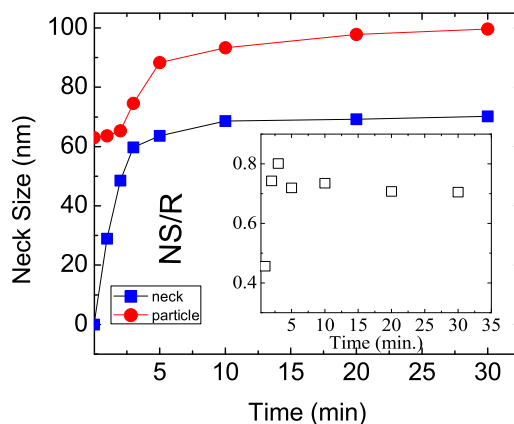


FIG. 3. (Color online) The neck size (square) and the particle diameter (circle) as a function of sintering time for Ag NPs sintered at 473K. Inset: the ratio of the neck size to the particle diameter.

tions. It is hence safe to deduce that excess sodium citrate contributes citrate anions which adsorb on the Ag NPs. The presence of Ag_2CO_3 in the pristine Ag NPs is possibly due to the decomposition of Ag-citrate complexes at 365 K.¹⁶ The further vaporization and decomposition of citrate complexes results in almost complete disappearance of the organic shells during sintering.^{12,16,18} However, the decomposition of Ag-citrate complexes is incomplete at the present sintering temperatures since citrate anions are detected even in Ag NPs sintered at 473 K.

Figure 3 presents the neck size and coalescence of Ag NPs as functions of time sintered at 473 K. The data are obtained by measuring about 20 particles from SEM images with IMAGE J software. The ratio between the neck and particle size is given in the inset. It is evident that the neck grows very fast until reaching 50% of particle size and then increases slowly. Meanwhile, Ag NPs do not dramatically coalesce in the initial fast neck growth. Figure 4 shows the tensile strength of bonded Cu wires to Cu pads with Ag NPs with a pressure of 5 MPa as a function of sintering temperatures. Cu pellet to pellet bonded with Ag metallo-organic compounds reported in Ref. 11 is also displayed for comparison. The dashed and dotted lines correspond to the tensile

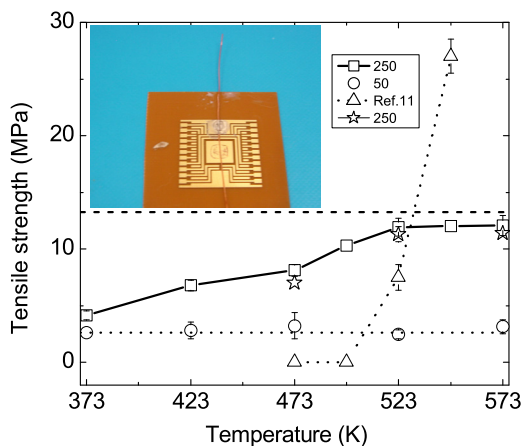


FIG. 4. (Color online) Tensile strength of bonded Cu wires to Cu pads with Ag NPs with a pressure of 5 MPa as a function of sintering temperatures. Data in Ref. 11 is also displayed for comparison. (circle) 50 μm Cu wires, (square) RT bonding strength of 250 μm wires cured at different temperatures, (pentagon) 250 μm wires cured at 150 $^\circ\text{C}$ while measured at elevated temperatures. Inset: bonded Cu wires to Cu pads on polyimide.

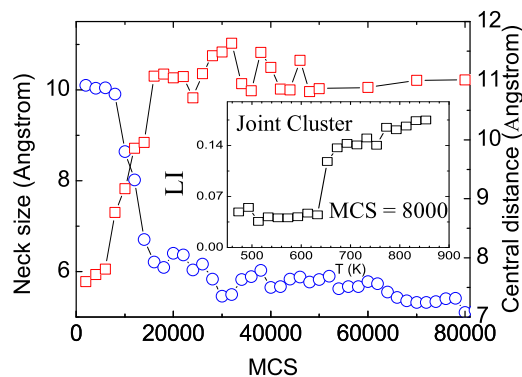


FIG. 5. (Color online) Neck size and the central distance plotted against MCS of two Ag55 clusters sintered at 473 K. Inset: Lindemann index of intermediate state of two Ag55 clusters sintered at a MCS of 8000.

strength of commercially available 50 and 250 μm wires, respectively. It is evident that the lowest bonding temperature is 373 K, at which the bonding is strong enough to break 50 μm wires. The formed 3D bonded network of Ag NPs provides global bonding through the Ag layers. For 250 μm wires, sintering at a higher temperature leads to an increase of bonding strength. The bonding is strong enough to break the wire after sintering at 523 K. It is obvious that the mechanical performance with condensing Ag NPs is better than that using Ag metallo-organic compounds since the present bonds are achieved at a lower temperature and a higher tensile strength is realized at the same sintering temperature. Instead of measuring at room temperature (RT) the bonding of the sample sintered at 423 K increases from 6.7 MPa (RT) to 7.1 MPa (473 K) when measured at 473 K and is able to break the wire again at 523 K. This indicates that sintering of Ag NPs continues and results in enhanced Ag NP bonding for working at a higher temperature.

To elucidate the underlying physics the sintering of two Ag NPs are simulated by Monte Carlo method with a tight-binding many-body potential.¹⁹ Figure 5 shows the neck growth and the central distance as a function of Monte Carlo step (MCS) for two Ag clusters, each with 55 atoms, sintered at 473 K. It is evident the initial growth of the neck is very fast, associated with the pronounced shrinkage of the central distance. This simulation is consistent with the experiments shown in Fig. 3.

The stability of joint clusters at individual intermediate state is theoretically studied through a further thermal sintering. The Lindemann index, relative root-mean-squared bond length fluctuation for the entire system,²⁰ was analyzed from 473 to 853 K with steps of 20 K. Such a result at MCS of 8000 is shown in the inset to Fig. 5. A step of the Lindemann index at 633 K is evident, which corresponds to the solid-liquid transition.^{20,21} The melting point of joint Ag110 clusters plotted against the central distance at intermediate states is shown in Fig. 6. It is clear that the sintering results in the increase of melting points of nanoscale clusters. This directly explains the data presented in Fig. 4, where samples sintered at 150 °C display an enhanced bonding strength when measured at a higher temperature.

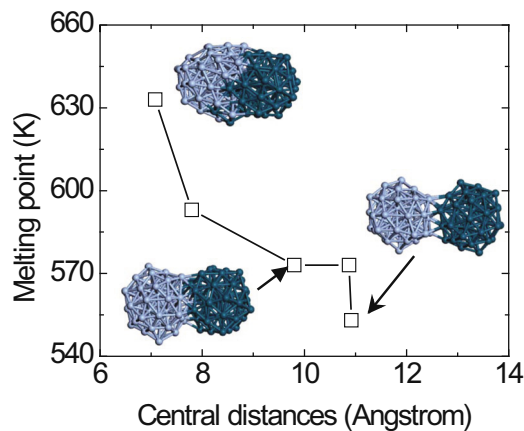


FIG. 6. (Color online) Melting points of two joint Ag55 clusters with different central distances. Inset figures are snapshots of intermediate sintering states.

In summary, we have developed a Ag NP paste for low temperature bonding. Robust bonding of Cu wire to Cu pads on polyimide has been achieved at 373 K through solid state sintering of Ag NPs and metallic bonding of Ag to Cu substrates. These bonds can withstand higher working temperatures through further sintering.

This work is partially supported by NSERC discovery grants, Canada, and NSFC, China (Grant No. 60725413).

- ¹Y. Lu, J. Y. Huang, C. Wang, S. Sun, and J. Lou, *Nat. Nanotechnol.* **5**, 218 (2010).
- ²Q. Cui, F. Gao, S. Mukherjee, and Z. Gu, *Small* **5**, 1246 (2009).
- ³E. Ide, S. Angata, A. Hirose, and K. F. Kobayashi, *Acta Mater.* **53**, 2385 (2005).
- ⁴S. H. Ko, H. Pan, C. P. Grigoropoulos, C. K. Luscombe, J. M. J. Frechet, and D. Poulidakos, *Nanotechnology* **18**, 345202 (2007).
- ⁵C. A. Lu, P. Lin, H. C. Lin, and S. F. Wang, *Jpn. J. Appl. Phys., Part 1* **46**, 4179 (2007).
- ⁶C. ö. Girit and A. Zettl, *Appl. Phys. Lett.* **91**, 193512 (2007).
- ⁷I. Mir and D. Kumar, *Int. J. Adhes. Adhes.* **28**, 362 (2008).
- ⁸T. Morita, E. Ide, Y. Yasuda, A. Hirose, and K. Kobayashi, *Jpn. J. Appl. Phys.* **47**, 6615 (2008).
- ⁹C. A. Lu, P. Lin, H. C. Lin, and S. F. Wang, *Jpn. J. Appl. Phys., Part 1* **45**, 6987 (2006).
- ¹⁰Y. C. Lin and J. Zhong, *J. Mater. Sci.* **43**, 3072 (2008).
- ¹¹Y. Akada, H. Tatsumi, T. Yamaguchi, A. Hirose, T. Morita, and E. Ide, *Mater. Trans.* **49**, 1537 (2008).
- ¹²H. Alarifi, A. Hu, M. Yavuz, and Y. Zhou, "Silver Nanoparticle Paste for Low-Temperature Bonding of Copper," *J. Electron. Mater.* (in press).
- ¹³K. Dick, T. Dhanasekaran, Z. Zhang, and D. Meisel, *J. Am. Chem. Soc.* **124**, 2312 (2002).
- ¹⁴NIST XPS DATA base, <http://srdata.nist.gov/xps/>.
- ¹⁵A. S. Tselesh, *Thin Solid Films* **516**, 6253 (2008).
- ¹⁶W. S. Epling, G. B. Hoflund, and G. N. Salaita, *J. Phys. Chem. B* **102**, 2263 (1998).
- ¹⁷G. N. Salaita, Z. F. Hazos, and G. B. Hoflund, *J. Electron Spectrosc. Relat. Phenom.* **107**, 73 (2000).
- ¹⁸H. Tada, J. Bronkema, and A. T. Bell, *Catal. Lett.* **92**, 93 (2004).
- ¹⁹F. Cleri and V. Rosato, *Phys. Rev. B* **48**, 22 (1993).
- ²⁰Y. Wen, Y. Zhang, J. Zheng, Z. Zhu, and S. Sun, *J. Phys. Chem. C* **113**, 20611 (2009).
- ²¹V. A. Mandelstam, P. A. Frantsuzov, and F. Calvo, *J. Phys. Chem. A* **110**, 5326 (2006).